The CDK inhibitor NtKIS1a is involved in plant development, endoreduplication and restores normal development of cyclin D3;1-overexpressing plants

Sophie Jasinski[1,‡], Catherine Riou-Khamlichi[2,*], Odile Roche[3], Claudette Perennes[1], Catherine Bergounioux[1] and Nathalie Glab[1]

[1]Laboratoire Cycle Cellulaire, Institut de Biotechnologie des Plantes, CNRS UMR8618, Université Paris-Sud, 91405 Orsay Cedex, France
[2]Institute of Biotechnology, University of Cambridge, Tennis Court Road, Cambridge, CB2 1QT, UK
[3]Service de Cytologie, Institut de Biotechnologie des Plantes, CNRS UMR8618, Université Paris-Sud, 91405 Orsay Cedex, France
*Present address: Institut des Sciences de la Vie et de la Santé, EA 3176, Université de Limoges, 87060 Limoges Cedex, France
‡Author for correspondence (e-mail: jasinski@ibp.u-psud.fr)

Accepted 3 December 2001
Journal of Cell Science 115, 973-982 (2002) © The Company of Biologists Ltd

Summary

Plant development requires stringent controls between cell proliferation and cell differentiation. Proliferation is positively regulated by cyclin dependent kinases (CDKs). Acting in opposition to CDKs are CDK inhibitors (CKIs). The first tobacco CKI (NtKIS1a) identified was shown to inhibit in vitro the kinase activity of CDK/cyclin complexes and to interact with CDK and D-cyclins. However, these features, which are common to other plant and animal CKIs already characterised, did not provide information about the function of NtKIS1a in plants. Thus, to gain insight into the role of NtKIS1a and especially its involvement in cell proliferation during plant development, we generated transgenic *Arabidopsis thaliana* plants that overexpress *NtKIS1a*. These plants showed reduced growth with smaller organs that contained larger cells. Moreover, these plants displayed modifications in plant morphology. These results demonstrated that plant organ size and shape, as well as organ cell number and cell size, might be controlled by modulation of the single *NtKIS1a* gene activity. Since in mammals, D-cyclins control cell cycle progression in a CDK-dependent manner but also play a CDK independent role by sequestering the CKIs p27^{Kip1} and p21^{Cip1}, we tested the significance of cyclin D-CKI interaction within a living plant. With this aim, *NtKIS1a* and *AtCycD3;1* were overexpressed simultaneously in plants by two different methods. Our results demonstrated that overexpression of the CKI *NtKIS1a* restores essentially normal development in plants overexpressing *AtCycD3;1*, providing the first evidence of cyclin D-CKI co-operation within the context of a living plant.

Key words: *Arabidopsis thaliana*, CDK inhibitor, Cyclin D, Endoreduplication, Plant development

Introduction

Developmental control of morphogenesis requires the co-ordination between cell proliferation, cell growth and cell differentiation. Because plant cells do not move and are surrounded by a rigid cell wall, a co-ordinated control of cell division is likely to be important in both environmental responses and developmental processes. Nonetheless, the mechanisms that link developmental events to the cell cycle machinery that controls cell proliferation remain poorly understood. Cell proliferation is precisely controlled by growth stimulatory and inhibitory signals transduced from the extracellular environment (Trehin et al., 1998). Cell cycle regulators such as CDKs, cyclins or CDK inhibitors integrate these signals. For example, D-cyclins are modulated by plant growth regulators and sucrose, and are thought to be important for stimulatory growth signal transduction between the environment and the cell cycle machinery (Meijer and Murray, 2000; Stals and Inze, 2001). Furthermore, expression of the CDK inhibitor *ICK1* is induced by abscisic acid, another growth regulator that prevents cell division (Wang et al., 1998).

In vertebrates, the existence of pathways linking development to cell cycle control was revealed by the occurrence of developmental defects that result from targeted mutation or overexpression of genes involved in cell cycle function, such as cyclin D or the retinoblastoma family (Cobrinik et al., 1996; Sicinski et al., 1995).

Because some of the inhibitory signals are believed to be mediated by CDK inhibitors, it is possible that these molecules contribute to cell cycle exit during differentiation. Consistent with this hypothesis, in double mutant mice lacking both functional p27^{Kip1} and p57^{Kip2}, or p21^{Cip1} and p57^{Kip2} CDK inhibitors, numerous cell types fail to differentiate during embryonic development (Zhang et al., 1998; Zhang et al., 1999). CDK inhibitors may also play a direct role in stimulating differentiation (Ohnuma et al., 1999). Although the signals that activate CKIs during differentiation remain unknown, these CKIs clearly provide a crucial link between cell-cycle arrest and differentiation (Myster and Duronio, 2000). In plants, activation of division by overexpressing *AtCycD3;1* or inhibition of division by overexpressing *ICK1* or *KRP2* induced profound effects on plant growth and development, providing a link between cell cycle regulation and development (De Veylder et al., 2001; Riou-Khamlichi et al., 1999; Wang et al., 2000).

Using a two-hybrid approach, we recently characterised the first tobacco CKI named *NtKIS1a*. Its deduced polypeptide sequence displayed strong similarity with plant CKIs and with the mammalian CDK inhibitor CIP/KIP family (S.J., C.B. and N.G., unpublished). The similarity between these proteins consists of a highly conserved domain similar to the CDK interaction/inhibition domain identified in the animal CIP/KIP inhibitors (Chen et al., 1996; Russo et al., 1996). Consistent with this, we showed that NtKIS1a inhibited the kinase activity of BY-2 cell CDK/cyclin complexes. In a two-hybrid system, NtKIS1a interacted with both CDK and D-cyclins but not with PCNA, suggesting that it was more closely related to $p27^{Kip1}$ than to $p21^{Cip1}$ (S.J., C.B. and N.G., unpublished).

In mammals, recent work indicates that the induction of cyclin D-CDK complexes results in a redistribution of CDK inhibitors $p27^{Kip1}$ and $p21^{Cip1}$ from cyclin E-CDK2 complexes to cyclin D-CDK4/6 complexes, thereby triggering the kinase activity of cyclin E-CDK2 (Sherr and Roberts, 1999). Thus, mammalian D-cyclins also control cell cycle progression in a kinase independent manner, via interaction with CIP/KIP.

In this study, we examined the effects of *NtKIS1a* overexpression on plant development. Gain of NtKIS1a function decreased organ size and increased cell size. Furthermore, it blocked the endoreduplication phenomenon. The significance of cyclin D-CKI interaction within the context of a living *Arabidopsis* was studied. With this aim, we took advantage of *AtCycD3;1*-overexpressing plants (Riou-Khamlichi et al., 1999), which had leaves curled along their proximal-distal axis and contained numerous small and incompletely differentiated cells (Meijer and Murray, 2001). We generated plants that overexpressed both *AtCycD3;1* and *NtKIS1a*. Analysis of these plants provided evidence for AtCycD3;1 and NtKIS1a interaction in planta.

Materials and Methods

Transgene constructs and *Arabidopsis thaliana* transformation

The full length cDNAs encoding *NtKIS1a* or *NtKIS1b* were cloned into pCW162. These plasmids were introduced into *Agrobacterium tumefaciens* (HBA10S). *Arabidopsis thaliana* plants, ecotype 'Columbia', were transformed with these constructions as previously described (Bechtold and Pelletier, 1998). Seeds from the *Agrobacterium*-treated plants were selected on 0.5× Murashige and Skoog medium containing 50 mg/l kanamycin (MS-Km). Kanamycin-resistant (Km^R) plantlets (T1) were transferred to soil in the greenhouse under long-day conditions (16 hours light) and the presence of the *NtKIS1a* or *NtKIS1b* cDNA was controlled by PCR. A study of the phenotype was carried out and the seeds were collected and plated onto MS-Km. 12 Km^R T2 plantlets from 20 T1 lines were transferred to the greenhouse and throughout their phenotype analysis we focused on four lines.

Transformation of *A. thaliana AtCycD3;1*-overexpressing plants was similarly performed, except that the *NtKIS1a* cDNA was cloned into Bin-Hyg-TX vector. Seeds from the *Agrobacterium*-treated plants were selected on MS-Km containing 25 mg/l hygromycin.

Genomic DNA extraction for PCR

Leaf fragments were ground in an extraction buffer (200 mM Tris-HCl, pH 7.5, 250 mM NaCl, 25 mM EDTA, 0.5% SDS). PCR, using the Promega TflI DNA polymerase, was performed in the presence of 2% DMSO on DNA from the isopropanol-precipitated supernatant.

RNA isolation and RT-PCR analysis

A. thaliana cauline leaves were frozen and ground in a mortar to perform total RNA extraction using TRIzol reagent (Life Technologies). For RT-PCR analysis, first-strand cDNA was synthesised from 5 μg of total RNA using SuperscriptII RNase H-Reverse Transcriptase (Life Technologies) following the manufacturer's instructions. 2.5 μl were used for PCR in a final volume of 25 μl. PCR products were then analysed on a 1% agarose gel and transferred onto a Hybond N+ membrane (Amersham). Hybridisations were performed at 62°C according to Church and Gilbert's protocol (Church and Gilbert, 1984). *NtKIS1a*, *AtCycD3;1* and *Actin2* probes correspond to the coding sequences.

Analyses by light and SEM microscopy

WT and 35S::NtKIS1a flowers were fixed with FAA (50% EtOH, 5% acetic acid, 10% formaldehyde), dehydrated in increasing ethanol concentrations and in propylene oxide and embedded in araldite resin for 60 hours at 48°C. 1.5 μm sections were cut with an LKB ultrotome III ultramicrotome, coloured with 0.5% toluidine blue and observed under a light microscope.

WT and 35S::NtKIS1a leaves of 1 cm were analysed with a scanning electron microscope (Hitachi S-3000N) under the ESED mode. Samples were slowly frozen at –12°C under partial vacuum on the Peltier stage before observation. Cell area was measured using the Optimas 6.0 software.

Flow cytometric analyses

Leaf fragments from WT, 35S::NtKIS1a and 35S::NtKIS1b plants were chopped in Galbraith's buffer (Galbraith et al., 1983). Mixtures were filtered and released nuclei were stained with Dapi and analysed using a flow cytometer (Vantage, Coulter).

Histone H1 kinase assay

$p9^{CKSHs1}$ beads were prepared as described (Azzi et al., 1992). *A. thaliana* plantlets (approximately 500 mg of fresh material) were ground in a mortar in liquid nitrogen with 1 ml of extraction buffer (25 mM MOPS pH 7.2, 60 mM β-glycerophosphate, 15 mM p-nitrophenylphosphate, 15 mM EGTA, 15 mM $MgCl_2$, 1 mM DTT, 1 mM NaF, 1 mM NH_4VO_3, 1 mM phenylphosphate, 0.2 μg/ml leupeptin, 0.3 μg/ml pepstatin). The resulting powder was slowly thawed on ice and centrifuged for 30 minutes at 18,000 ***g*** at 4°C to eliminate cell debris. Protein extract (570 μg) was added to 10 μl of packed $p9^{CKSHs1}$ beads previously washed three times with bead buffer (Azzi et al., 1992) and kept under rotation at 4°C for 1 hour 30 minutes. After a centrifugation pulse and removal of the supernatant, beads were washed three times with bead buffer and used for H1K assays. Samples containing the initial 10 μl packed beads were incubated for 30 minutes at 30°C with 1 μCi[γ-^{32}P]ATP, 25 μg histone H1 (Sigma) in a final volume of 30 μl H1K assay buffer (Azzi et al., 1992). The reaction was stopped by placing samples on ice. After a centrifugation pulse, Laemmli buffer was added to 15 μl of supernatant. Samples were analysed by 12% SDS-PAGE followed by Coomassie blue staining to visualise histone H1 and autoradiography to detect histone H1 phosphorylation, which was further quantified with the NIH image 1.62 software.

Western blotting

After H1K assays, proteins bound to $p9^{CKSHs1}$ beads were recovered by boiling in the presence of Laemmli buffer, run on 12% SDS-PAGE gels and transferred to a 0.1 μm nitrocellulose membrane for 1 hour in a semi-dry system (Millipore) at 2.5 V/cm^2. The membrane was further treated as described in the ECL+Plus System protocol (Amersham). The primary antibody was a monoclonal anti-PSTAIR

antibody (Sigma), and the secondary one was a goat anti-mouse peroxidase conjugated antibody (BioRad). Detection of the target proteins was performed by chemoluminescence using the ECL+Plus System (Amersham).

Yeast two-hybrid assays

Yeast two-hybrid assays were performed according to the protocol described in the Matchmaker Two-Hybrid system (Clontech).

Results

The overexpression of the CDK inhibitor NtKIS1a induces serrated leaves and abnormal flowers

To examine the roles of NtKIS1a on plant growth and development, *A. thaliana* transgenic lines in which the *NtKIS1a* cDNA was expressed under the control of the constitutive cauliflower mosaic virus 35S promoter were generated. *NtKIS1b* cDNA, a spliced variant expressed in planta, was used as control. NtKIS1b did not interact with A-type CDK nor with D-type cyclins and did not inhibit the kinase activity of CDK/cyclin complexes (S.J., C.B. and N.B., unpublished). The presence of the *NtKIS1a* or *NtKIS1b* cDNAs was controlled on genomic DNA in the Kanamycin-resistant (Km^R) T1 plantlets and their effective expression was monitored using RT-PCR analyses. The 35S::NtKIS1b T1 plants displayed no significant difference compared with WT plants (Fig. 1A,d,e). By contrast, 40% (16 from 40 independent lines) of 35S::NtKIS1a T1 plants showed phenotypic modifications. Serrated and/or undulated leaves were observed in all the 16 plants. However, we noticed a gradient in the undulation, the depth and the number of the teeth with deeper and more numerous teeth in the strongest phenotype. Fig. 1Aa,b,c represented rosette leaves, referred to as weak, medium and strong phenotypes, respectively. Not only was the leaf margin affected, but also the rosette diameter was reduced, as measured in the next generations (Fig. 1B). Compared with wildtype (WT), the flowering time was advanced in several lines (not shown). Furthermore, in five lines that harboured the strong leaf phenotype (Fig. 1A,c), flowers were smaller and did not give seeds (Fig. 1A,f,g). The phenotype of these lines, which were lost, was referred to as 'extreme' in the text.

The T2 progeny of four T1 lines (one displaying a strong, one displaying a medium, and two displaying no significant or a weak phenotype) was analysed. According to the number of T2 plants displaying a serrated leaf phenotype, three cases were observed. In the first case, which described the progeny of a T1 strong line, 12 plants out of 12 grown, presented the serrated phenotype with a gradient in the depth of the teeth. Among these 12 plants, 5 displayed a more severe phenotype than the T1 parents, were affected in flower morphology and were sterile. In the second case, which described the progeny of a T1 medium line, 8 plants out of 12 were affected in leaf morphology but remained fertile. Finally, in the third case, which described the progeny of a weak T1 line, only 1 plant out of 12 T2 presented serrated leaves and was fertile (Fig. 1C). The number of T2 plants that displayed a serrated phenotype was assumed to reflect the disjunction of the transgene insertions present in the T1 parents. Interestingly, we observed stronger phenotypes when there were more T2 plants affected (Fig. 1C). Consequently, it was suggested that the strength of

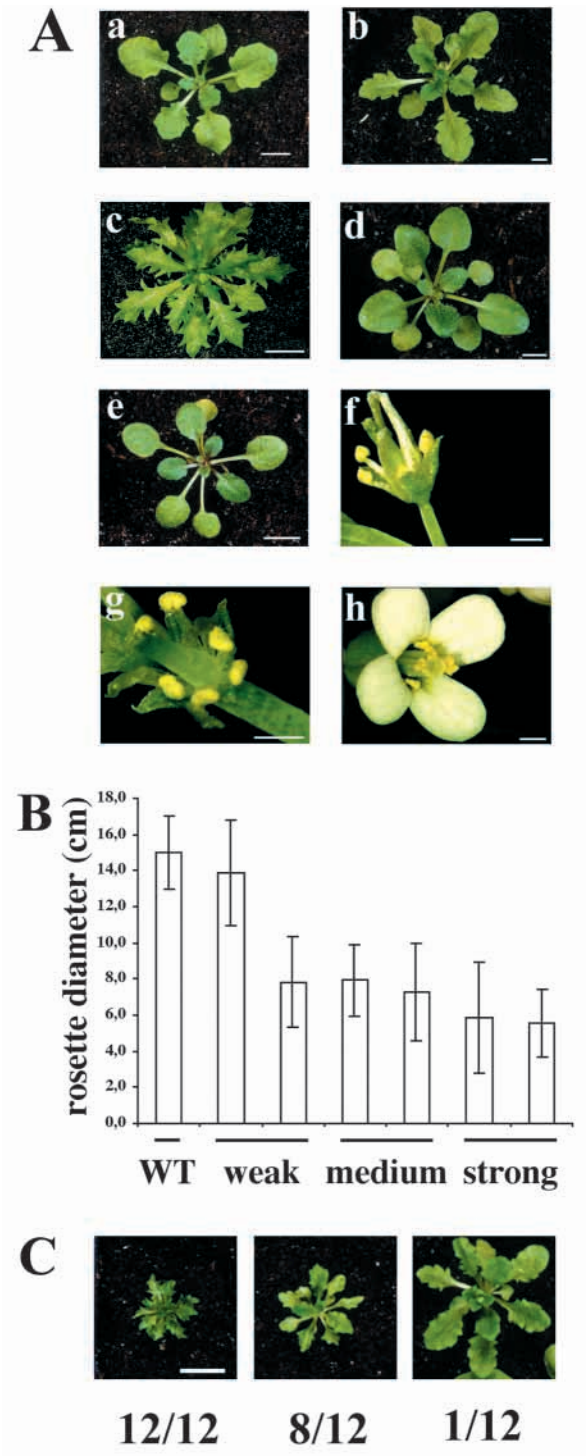

Fig. 1. Gain of function of NtKIS1a produces serrated leaves, abnormal flowers and reduces plant size. (A) Rosettes from three T1 35S::NtKIS1a independent lines, displaying respectively a weak (a), medium (b) and strong (c) serrated leaf phenotype, are compared with 35S::NtKIS1b (d) or WT (e) rosette. Abnormal flowers from 35S::NtKIS1a line displaying an extreme phenotype (f,g; see text) are compared with WT flower (h). Bars, 5 mm (a-e); 0.5 mm(f-h). (B) The rosette diameter of 24 plants (5-week-old) from 2 weak, 2 medium and 2 strong lines were measured. The graph represents the average diameter ± s.d. (C) Three cases were met according to the number of T2 plants displaying a serrated leaf phenotype in 12 Km^R plants analysed. For each case, a serrated plant is shown. Bar, 10 mm.

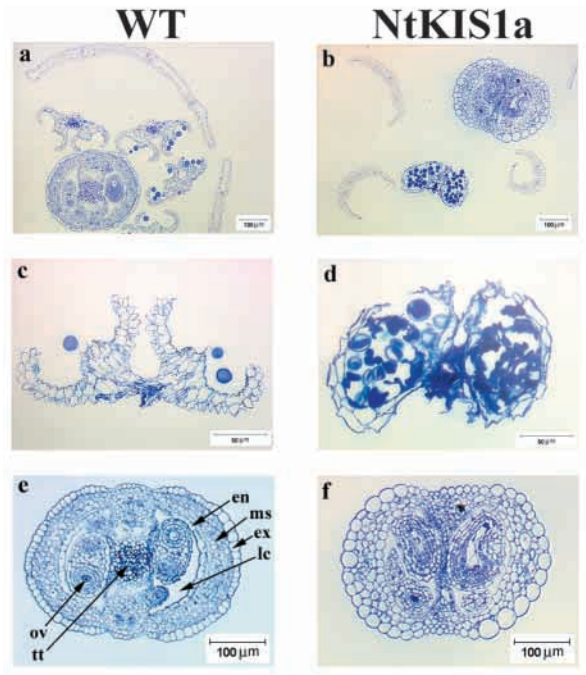

Fig. 2. *NtKIS1a* overexpression induces anther and gynoecium disorganised structure. Transverse sections of flowers from wildtype (WT) or a 35S::NtKIS1a line displaying an extreme phenotype (NtKIS1a) were performed. a and b corresponded to general views. More detailed views of anthers (c,d) and ovaries (e,f) are shown. In WT ovary, exocarp (ex), mesocarp (ms), and endocarp (en) layers could be distinguished. The dark staining cells of the transmitting tract (tt) occupied the inner portion of the ovary. Inside the locules (lc), ovules (ov) were visible in WT and NtKIS1a.

the phenotype was to some extent related to the number of transgene insertions.

Closer inspection of the extreme flower phenotype showed a conservation of all the whorls with, however, a reduced growth of petals and stamens (Fig. 1A,f,g). To understand the reasons for the sterility, flower transversal sections of WT and 35S::NtKIS1a were compared (Fig. 2). In 35S::NtKIS1a anthers, pollen grains were formed. Nevertheless, they showed a strong heterogeneity in size. Furthermore, the anthers had a disorganised structure and failed to dehisce (Fig. 2b,d). The gynoecium structure was also affected (Fig. 2f). Its organisation in three layers, exo, meso and endocarp, was not clearly observed compared with the WT (Fig. 2e). Moreover, most of the cells were enlarged and their shape seemed to be modified. Additionally, the transmitting tract, a tissue specialised in directing pollen tube growth, was nearly absent in 35S::NtKIS1a. The ovules displayed a disorganised structure but were apparently not affected in number.

35S::NtKIS1a plants show reduced CDK kinase activity

The CDK kinase activity was analysed in two 35S::NtKIS1a lines, one strong and one medium. Results shown in Fig. 3 demonstrated that the CDK kinase activity measured in these lines was significantly decreased compared with WT. Moreover, since 60% inhibition was observed in strong line and 37% in the medium one, it suggested that the CDK kinase activity inhibition was correlated to the strength of the phenotype.

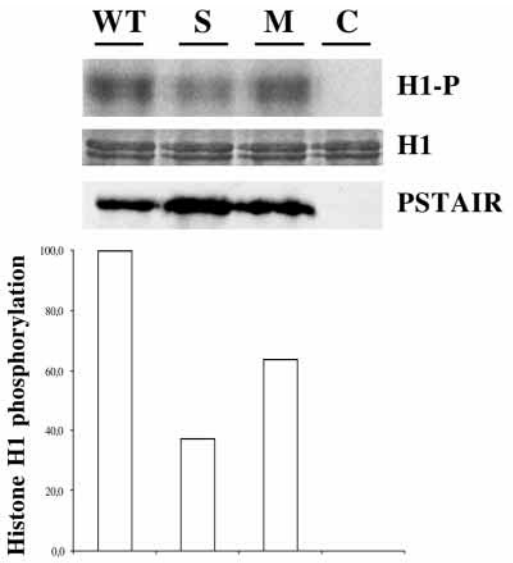

Fig. 3. The CDK kinase activity of 35S::NtKIS1a lines is reduced. Protein extracts from wildtype (WT), two 35S::NtKIS1a *Arabidopsis* lines, one strong (S) and one medium (M), or buffer (C) were added to p9^{CKSHs1} beads to purify CDK/cyclin complexes. Histone H1 phosphorylation (H1-P) was monitored and equal loading of histone H1 (H1) was controlled. Proteins bound to p9^{CKSHs1} beads were recovered and immunoblotted with an antibody raised against the conserved CDK PSTAIR motif (PSTAIR). The histone H1 phosphorylation and the PSTAIR signals were quantified with NIH image 1.62 software. Their ratio was calculated and presented in the graph. The maximal value obtained in WT was referred as 100%.

Gain of NtKIS1a function in *Arabidopsis* plants decreases organ size and increases cell size

The decrease in plant and organ size observed in the 35S::NtKIS1a lines could reflect an alteration in cell size and/or cell number. To investigate this last point at the cellular level, we examined the size of cells in 35S::NtKIS1a petals and leaves in comparison with the wildtype (Fig. 4). In WT petals, the shape and size of the cells were different along the organ and defined three regions: basal (III), median (II) and distal (I) (Fig. 4A,B). In the basal and median regions, the cells had a lengthened shape, basal cells being larger than median cells, whereas in the distal region, cells had a round shape and a small size. Interestingly, in the 35S::NtKIS1a, the cells had a constant lengthened shape all along the petal. The distal cells were still smaller than the basal cells but had lost their round shape. Moreover, the petal margin was serrated (Fig. 4B). Comparison of cells from WT and 35S::NtKIS1a demonstrated that the cell size at all three regions was significantly increased in the outer epidermis of 35S::NtKIS1a petals (Fig. 4C). Since 35S::NtKIS1a petals were smaller, it suggested that petals had fewer cells per organ than the WT.

The size of leaf lower epidermis cells from two 35S::NtKIS1a lines was analysed using scanning electron microscopy and the cell area was further quantified using the optimas 6.0 software. The results show that the cells were significantly enlarged in *NtKIS1a*-overexpressing plants compared with a WT plant (Fig. 4D). In WT, cell area varied from 180 to 3516 μm^2 and three categories of

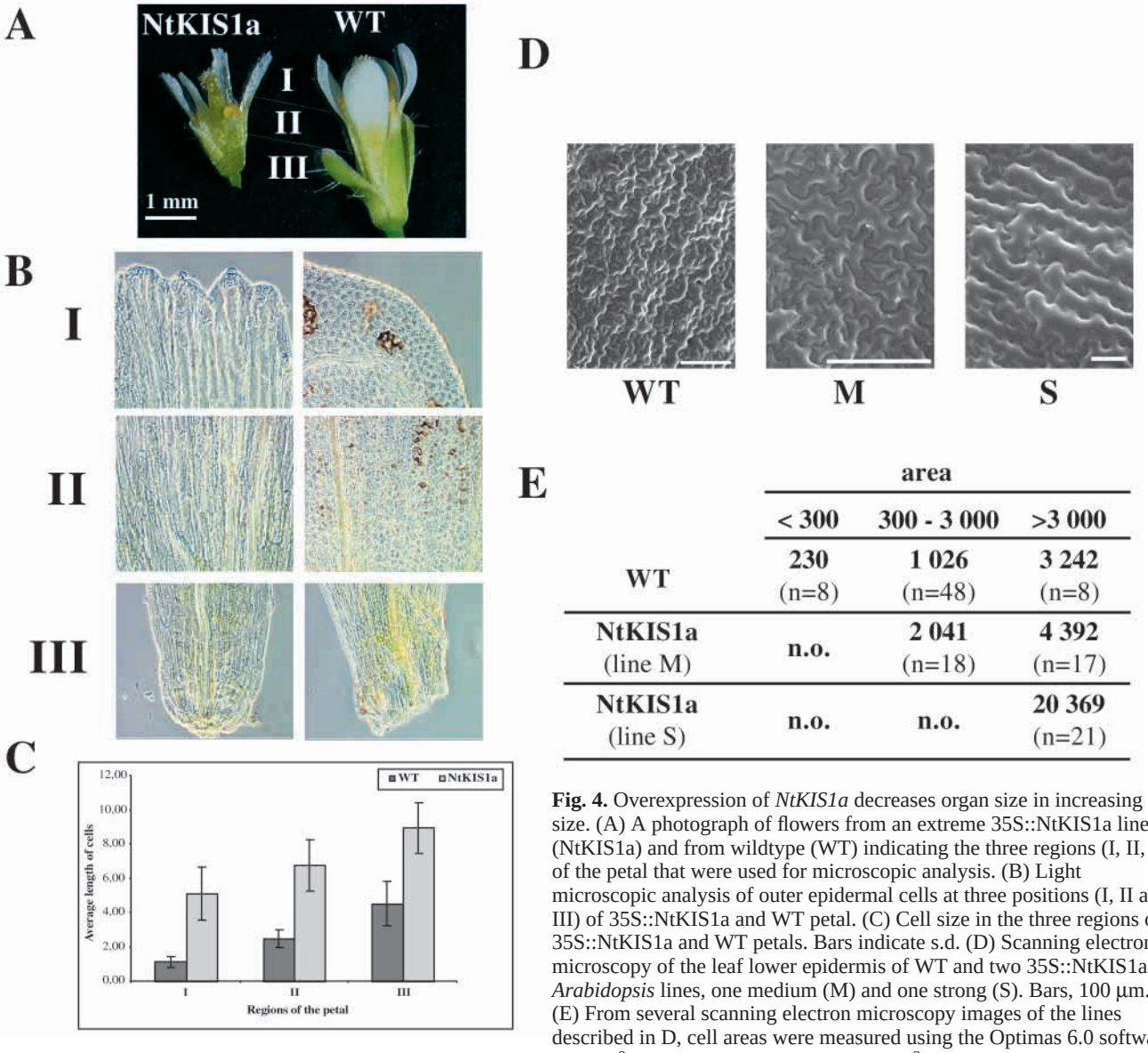

E

	area		
	< 300	300 - 3 000	>3 000
WT	230 (n=8)	1 026 (n=48)	3 242 (n=8)
NtKIS1a (line M)	n.o.	2 041 (n=18)	4 392 (n=17)
NtKIS1a (line S)	n.o.	n.o.	20 369 (n=21)

Fig. 4. Overexpression of *NtKIS1a* decreases organ size in increasing cell size. (A) A photograph of flowers from an extreme 35S::NtKIS1a line (NtKIS1a) and from wildtype (WT) indicating the three regions (I, II, III) of the petal that were used for microscopic analysis. (B) Light microscopic analysis of outer epidermal cells at three positions (I, II and III) of 35S::NtKIS1a and WT petal. (C) Cell size in the three regions of 35S::NtKIS1a and WT petals. Bars indicate s.d. (D) Scanning electron microscopy of the leaf lower epidermis of WT and two 35S::NtKIS1a *Arabidopsis* lines, one medium (M) and one strong (S). Bars, 100 μm. (E) From several scanning electron microscopy images of the lines described in D, cell areas were measured using the Optimas 6.0 software. The mean cell areas were reported in three categories: areas less than 300 μm^2, areas between 300 and 3000 μm^2 and areas greater than 3000 μm^2 (n.o. correspond to categories not observed). The number of cells (n) recorded in each categories is indicated in brackets.

cell area can be described: area less than 300 μm^2; area between 300 and 3000 μm^2; and area greater than 3000 μm^2 (Fig. 4E). In the 35S::NtKIS1a line displaying a medium phenotype, cells with an area less than 300 μm^2 were never observed. Additionally, in the two remaining groups, the average cell area was increased. In the 35S::NtKIS1a line displaying a strong phenotype, only cells with an area greater than 3000 μm^2 were observed, on average 6.3-fold higher than the corresponding cell area in the WT (Fig. 4E).

Rosette leaves of 35S::NtKIS1a plants display a decreased DNA content

Most *Arabidopsis* organs consist of cells with polyploid nuclei attributable to endoreduplication, which increases cell size (Bergounioux et al., 1992; Koornneef, 1994). Since an increase in size was revealed in 35S::NtKIS1a plant cells, the ploidy level in different organs of 35S::NtKIS1a, 35S::NtKIS1b and WT plants was compared by flow cytometric analysis. In rosette leaf cells of WT plants, the maximal endoreduplication level reached 64C, the proportion of cells with a high DNA content increased with leaf aging, as already observed (S.C. Brown, personal communication). Conversely, the distribution pattern of DNA content in cauline leaves was modified and reached a 2C and 4C distribution in flower buds. Surprisingly, in 35S::NtKIS1a plants displaying a strong phenotype, cells of all the tested organs, even the rosette leaves, displayed a 2C and 4C DNA content distribution (Fig. 5). This result demonstrated that the endoreduplication phenomenon was absent in these 35S::NtKIS1a plants. Moreover, in these plants, the proportion of 4C DNA content cells was very low resulting in an overwhelming 2C DNA content cell population.

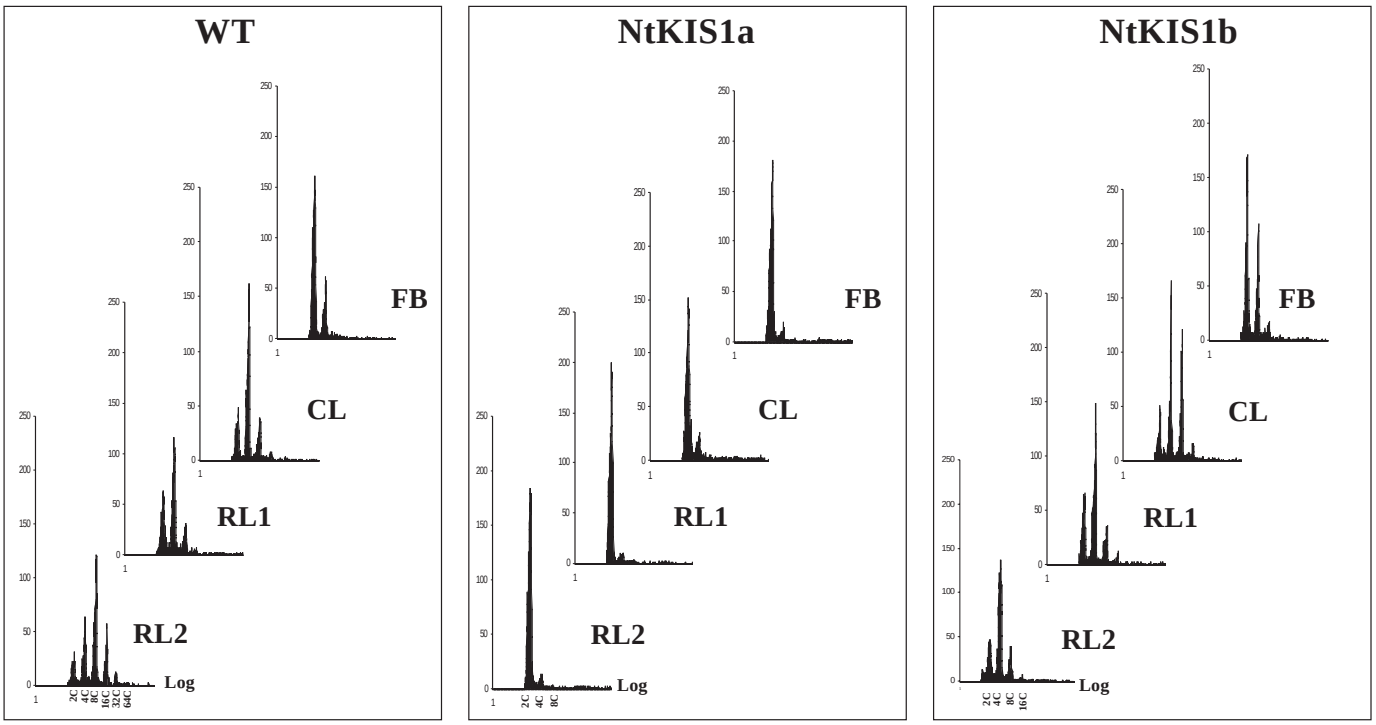

Fig. 5. Overexpression of *NtKIS1a* inhibits rosette leaf cell endoreduplication. Ploidy distributions for nuclei isolated from old (RL2) and young (RL1) rosette leaves, cauline leaves (CL) and flower buds (FB) of *A. thaliana* wildtype (WT), strong 35S::NtKIS1a (NtKIS1a) or 35S::NtKIS1b (NtKIS1b) lines. For each sample, 5000 DAPI-stained nuclei were analysed. The *x*-axis represents DNA fluorescence in logarithmic scale and DNA content is indicated. The *y*-axis represents frequency.

Overexpression of *NtKIS1a* rescues normal development in *AtCycD3;1*-overexpressing plants

The flow cytometric analysis performed on *NtKIS1a*-overexpressing *Arabidopsis* plants suggested that NtKIS1a prevents endoreduplication and may influence S phase progression. Therefore, to gain more insight into the various pathways in which NtKIS1a could be involved we first hypothesised that it might interact with D-cyclin/CDK complexes. Indeed, we previously showed that NtKIS1a interacts with tobacco D-cyclins in a yeast two-hybrid system (S.J., C.B. and N.G., unpublished). Additionally, the *Arabidopsis* D-cyclin AtCycD3;1 represented one of the preys obtained in a two-hybrid screen using NtKIS1a as a bait (S.J., C.B. and N.G., unpublished). This interaction was further confirmed (Fig. 6A), demonstrating that these two proteins were interacting partners in a two-hybrid system. In *Arabidopsis*, *AtCycD3;1* overexpression resulted in the formation of abnormal plants that contained numerous small, incompletely differentiated cells (Meijer and Murray, 2001). Moreover, these plants showed disorganised meristem, late flowering and delayed senescence (Riou-Khamlichi et al., 1999).

To determine whether NtKIS1a could inhibit the CDK/cyclin D3;1 activity and thus rescue the *AtCycD3;1*-overexpression phenotype, NtKIS1a and AtCycD3;1 were combined in the context of a living *Arabidopsis* plant by two different methods. First, we performed hand-pollination of *AtCycD3;1* pistils with *NtKIS1a*-overexpressing pollen. The presence of both *AtCycD3;1* and *NtKIS1a* transgenes was controlled in F1 plants by PCR analysis (not shown) and their effective overexpression was checked by RT-PCR (Fig. 6B, left). Interestingly, the phenotype of the AtCycD3;1×NtKIS1a plants was similar to that of the WT, making clear differences to those observed in both *AtCycD3;1* or *NtKIS1a*-overexpressing plants (Fig. 6C, top). Indeed, both serration and/or undulation and curling of leaves, associated with *NtKIS1a* and *AtCycD3;1* overexpression, respectively, disappeared in the crossed plants. Closer inspection of the restored phenotype was performed by scanning electron microscopy of leaf lower epidermis cells. Cell area measurement revealed that the three groups, previously described for WT plants (Fig. 4), were also represented in the AtCycD3;1×NtKIS1a plants (Fig. 6D). Indeed, in the crossed plants, cells with an area greater than 300 μm^2 reappeared compared with 35S::AtCycD3;1 plants and, reciprocally, cells with an area less than 3000 μm^2 reappeared compared with 35S::NtKIS1a plants (Fig. 4E; Fig. 6D). These results suggested an in vivo functional co-operation between these two cell cycle regulators.

Second, the *AtCycD3;1*-overexpressing line was transformed with the *NtKIS1a*-containing transgene, resulting in double overexpressing plants. The presence of the *NtKIS1a* transgene was controlled on genomic DNA in the Kanamycin-resistant (Km^R) T1 plantlets (AtCycD3;1+NtKIS1a) and its effective expression was monitored through RT-PCR analyses (Fig. 6B, right). As previously observed for crossed plants, double transformants displayed a WT-like phenotype (Fig. 6C, bottom). At the level of leaf lower epidermis cell area, the AtCycD3;1+NtKIS1a plants displayed a distribution similar to that found in crossed plants (not shown). Furthermore, the double transformed plants had an advanced flowering time

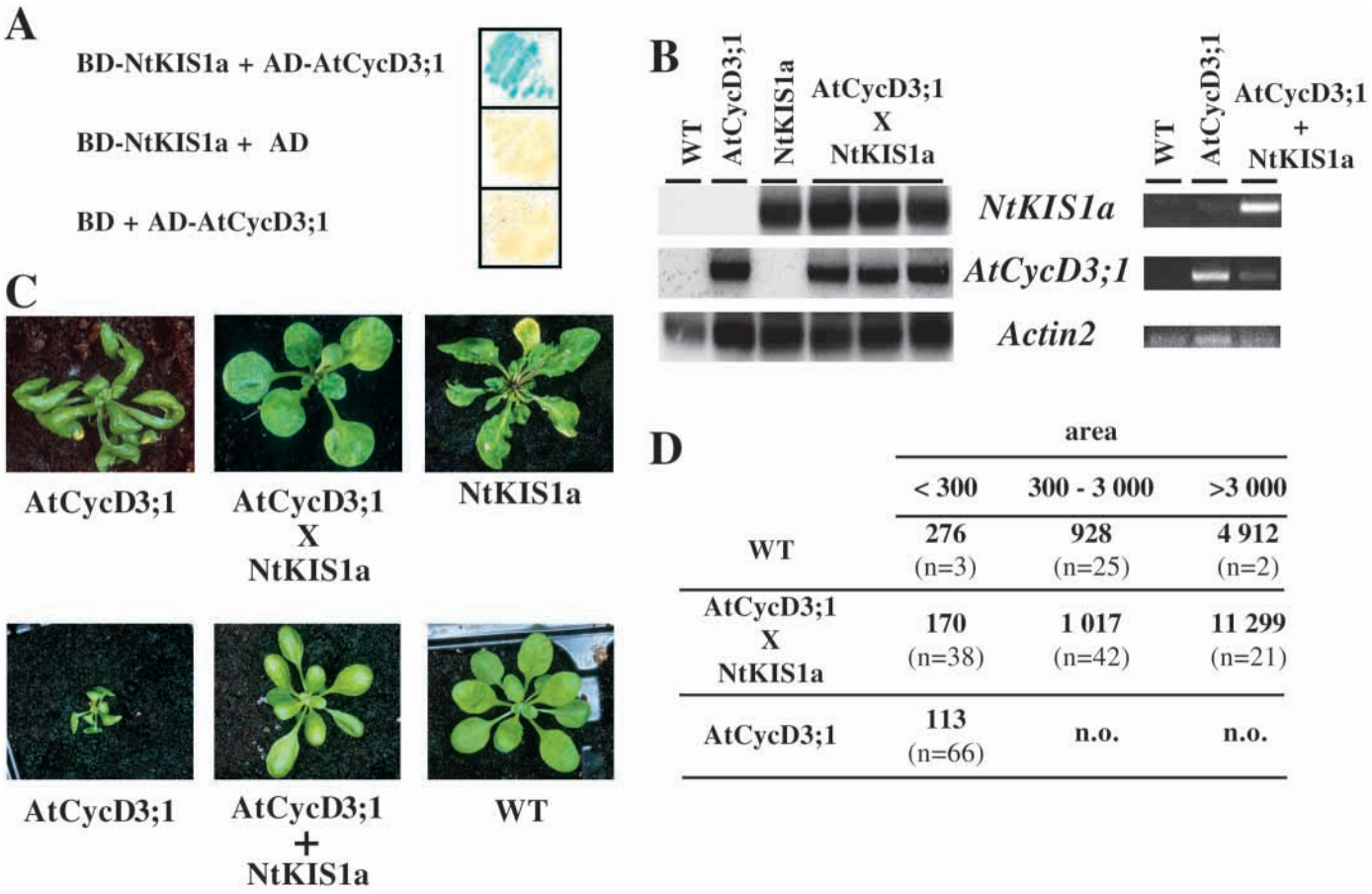

D

	area		
	< 300	300 - 3 000	>3 000
WT	276 (n=3)	928 (n=25)	4 912 (n=2)
AtCycD3;1 X NtKIS1a	170 (n=38)	1 017 (n=42)	11 299 (n=21)
AtCycD3;1	113 (n=66)	n.o.	n.o.

Fig. 6. *A. thaliana* plants overexpressing *NtKIS1a* and *AtCycD3;1* display a wildtype phenotype. (A) The interaction between NtKIS1a and AtCycD3;1 using the two-hybrid system is presented. BD-NtKIS1a corresponds to the DNA binding domain of GAL4 fused to NtKIS1a and AD-AtCycD3;1 corresponds to the activation domain of GAL4 fused to AtCycD3;1. AD and BD correspond respectively to the activation and DNA binding domains of GAL4. (B) RT-PCR analysis was performed as described in Materials and Methods. Lanes WT, AtCycD3;1, NtKIS1a, AtCycD3;1×NtKIS1a and AtCycD3;1+NtKIS1a are RT-PCR products obtained from RNA samples of the corresponding plants. AtCycD3;1×NtKIS1a correspond to the F1 plants of the cross between the AtCycD3;1 and NtKIS1a-overexpressing lines. AtCycD3;1+NtKIS1a correspond to T1 plants issued from the transformation of the AtCycD3;1-overexpressing line by the NtKIS1a-containing transgene. Three independent plants were tested for AtCycD3;1×NtKIS1a. PCR was performed with specific primers from *NtKIS1a* (first row), *AtCycD3;1* (second row) and *Actin2* (third row; used as control), respectively. (C) Top row: view of a 6-week-old plantlet from the *AtCycD3;1*-overexpressing line (AtCycD3;1), and view of 4-week-old plantlets from 35S::NtKIS1a (NtKIS1a) and AtCycD3;1×NtKIS1a lines. Bottom row: view of 3-week-old plantlets from *AtCycD3;1*-overexpressing line (AtCycD3;1), AtCycD3;1+NtKIS1a and WT. (D) From several scanning electron microscopy images of the lines described in C, bottom row, cell areas were measured using the Optimas 6.0 software. The averages of cell areas were reported in three categories, as described in the legend of Fig. 4. The measurement presented here for WT is an independent measurement of the WT measurement shown in Fig. 4.

compared with the flowering time of the 35S::AtCycD3;1 plants (Riou-Khamlichi et al., 1999) (not shown).

Since a wildtype-related phenotype was recovered through the combination of NtKIS1a and AtCycD3;1 by two independent manners, it strongly suggested that these two proteins, in addition to being two-hybrid interacting partners, co-operated in planta to restore a pseudo wildtype balance of their opposite activities towards cell cycle progression.

Discussion

Gain-of-function of NtKIS1a inhibits CDK kinase activity, cell division and disturbs plant morphology

Introduction of the tobacco CDK inhibitor NtKIS1a in *Arabidopsis* generated phenotypic modifications in several transgenic lines. Their phenotypic analysis demonstrated that the gain of function of NtKIS1a in *Arabidopsis* was correlated with an alteration of organ morphology (serration and/or undulation) together with a reduced plant growth, which resulted from the decrease in organ size (Fig. 1). In addition, 35S::NtKIS1a leaves contained larger cells than WT (Fig. 4) and our results indicated that more profound morphological alterations were associated with larger cells. Furthermore, in 35S::NtKIS1a extreme lines, organs such as petals, ovaries or anthers contained larger cells than in WT organs (Figs 2, 4). As a consequence of these observations, smaller organs must contain fewer cells. These results strongly suggested that NtKIS1a activity was sufficient to control organ and cell size as well as cell number. Since, cell number is determined primarily by cell division, the negative correlation between *NtKIS1a*

overexpression and organ cell number established that NtKIS1a, previously shown in vitro to be a CDK inhibitor (S.J., C.B. and N.G., unpublished), was also a negative regulator of cell division in planta. Indeed, it was confirmed that the kinase activity in 35S::NtKIS1a lines was strongly reduced, the level of inhibition being related to the strength of the phenotype (Fig. 2). The absence of phenotype in plants transformed with NtKIS1b, the NtKIS1a variant lacking inhibitory properties in vitro, correlated perfectly with the previous conclusions that established NtKIS1a as a negative cell cycle regulator. In mammals, $p27^{Kip1}$ was demonstrated to be a potent negative regulator of cell proliferation since mice lacking $p27^{Kip1}$ displayed enlarged organs that contained more cells (Fero et al., 1996). The decrease in cell number together with an increase in cell size in 35S::NtKIS1a organs may be viewed either as resulting from uncoupling of cell growth and cell division or as a direct correction by the morphogenetic programme to compensate for lack of cells (Meijer and Murray, 2001). Gain-of-function of the CDK inhibitor NtKIS1a was also associated with modifications in plant morphology, such as serration of leaves and petals (Figs 1, 4). This result suggested that plant organ shape could be disturbed solely by modulation of the *NtKIS1a* gene activity. Interestingly, overexpression of the *Arabidopsis* CKIs, *ICK1* (Wang et al., 2000), *KRP2* and *KRP3* (De Veylder et al., 2001), produced plant modifications closely related to overexpression of *NtKIS1a*. This suggested that the phenotypes observed reflected an overall effect of the constitutive overexpression of $p27^{Kip1}$-like CDK kinase inhibitors in *A. thaliana*, regardless of their specific function.

It was previously shown that depth of toothing or lobing could be affected by alteration of gibberellin levels (Chandra Sekhar and Sawhney, 1991). Investigation of such a relationship between NtKIS1a and gibberellins should be helpful to understand how *NtKIS1a* overexpression impaired leaf morphogenesis. Interestingly, there was a gradient in the strength of the serrated phenotype with deeper teeth in the strongest phenotype. Gradual modifications were observed in the T1 generation between normal plants, which were fertile and displayed only weakly serrated leaves, and the tiny extremely serrated plants displaying sterile flowers with short petals and non dehiscent anthers. It is important to note that abnormal flowers were never observed without strongly serrated leaves. It suggested that affecting cell division in petals required higher level of CKIs activity than needed for modifying leaf shape and size. Indeed, the analysis of the transgene disjunction demonstrated that the extreme phenotype affecting both leaves and flowers was only found in the strong T1 lines, where all the T2 progeny presented a serrated phenotype (Fig. 1C). It suggested that only the plants containing the highest number of transgene copies were affected in flowers. Remarkably, in 35S::NtKIS1a plants, all organs were formed with the right identity. Therefore, despite *NtKIS1a* being expressed under the constitutive 35S promoter, it did not interfere with identity acquisition of meristems nor organs. NtKIS1a would preferentially act at terminal differentiation of the plant organ cells since only the morphogenesis of organs was affected.

Cell size and endoreduplication

There is a large body of evidence indicating that the final size of a cell is linked to its DNA content (Traas et al., 1998). In 35S::NtKIS1a rosette leaves, cells displayed a 2C and 4C DNA content distribution (Fig. 5), demonstrating that the endoreduplication phenomenon, known to occur in the WT rosette, was affected. Interestingly, in the 35S::NtKIS1a plants, which displayed a strong serrated phenotype, endoreduplication was completely prevented (Fig. 5), whereas this block was only partial in less affected plants (medium and weak lines, not shown). This result demonstrated that the NtKIS1a CDK inhibitor interfered with the endoreduplication phenomenon in *Arabidopsis* when overexpressed. However, these results did not provide information towards the involvement of NtKIS1a in endoreduplication in tobacco. Surprisingly, the endoreduplication block observed in *NtKIS1a*-overexpressing *Arabidopsis* was accompanied with a phenomenal cell enlargement: 6.3-fold in the strong lines in which the endoreduplication block was complete (Figs 4, 5). It demonstrated that, in 35S::NtKIS1a *Arabidopsis* rosette leaves, endoreduplication and cell size could be uncoupled.

Endoreduplication and differentiation

Endoreduplication is the major mechanism leading to somatic polyploidisation in plants and has been described in many specific cell types that are highly specialised (Joubes and Chevalier, 2000). This phenomenon represents a growing field of interest in plant biology as it characterises the switch between cell proliferation and cell differentiation during developmental steps. Endoreduplication shares several characteristics with the mitotic cycle. In particular, the endoreduplicative cycle appears to be under control of the same CDK/cyclin complexes. However, both cycles are mutually exclusive and higher eukaryotes have developed strategies that ensure an inhibition of endoreduplication during mitosis and vice versa (Larkins et al., 2001). A variety of biological processes, especially cell differentiation, have been proposed to involve endoreduplication (Joubes and Chevalier, 2000). However, the role and the control of the endocycle are poorly characterised in plants. Interestingly, since two plant CKIs [*NtKIS1a* (this paper) and *KRP2* (De Veylder et al., 2001)] prevented endoreduplication when overexpressed, it suggested that CKIs could be potent regulators of this phenomenon in *Arabidopsis*. Similarly, in *Caenorhabditis elegans*, it was suggested that the CDK inhibitor CKI-1 might play a role in endoreduplication, since it was expressed in differentiated intestinal cells that underwent endoreduplicative cell cycles (Hong et al., 1998). In mammals, $p57^{Kip2}$ is involved in the transition to the endocycle in trophoblast giant cells during terminal differentiation and interestingly, ectopic expression of a stabilised $p57^{Kip2}$ mutant protein blocked endoreduplication (Hattori et al., 2000). Furthermore, the mutation of the CDK and cyclin binding domains of $p57^{Kip2}$ abrogated its inhibitory activity on endoreduplication when overexpressed (Hattori et al., 2000). Consistent with this, endoreduplication occurred in plants overexpressing *NtKIS1b* (Fig. 5), which lacked the C-terminal end, necessary for both CDK and cyclin interaction (S.J., C.B. and N.G., unpublished).

NtKIS1a and cyclin D3;1 interaction

In mammals, D-cyclins are thought to drive cell cycle

progression by associating with their CDK partners (CDK4 and CDK6) and by guiding these kinases to their cellular substrates (Sherr, 1995). In addition to their well-documented CDK-dependent role, D-cyclins play a kinase independent function by sequestering cell cycle inhibitors $p27^{Kip1}$ and $p21^{Cip1}$, thereby triggering the kinase activity of cyclin E-CDK2 (Sherr and Roberts, 1999). Moreover, in the context of a living mouse, the significance of cyclin D1-$p27^{Kip1}$ interaction was demonstrated, since deletion of $p27^{Kip1}$ rescues developmental abnormalities of cyclin D1-deficient mice (Geng et al., 2001; Tong and Pollard, 2001). NtKIS1a was shown to interact with tobacco and *Arabidopsis* D-cyclins (S.J., C.B. and N.G., unpublished) (Fig. 6A), known as positive regulators of the cell cycle machinery (De Veylder et al., 1999; Riou-Khamlichi et al., 1999; Riou-Khamlichi et al., 2000). In order to address the significance of cyclin D-NtKIS1a interaction in the context of a living *Arabidopsis*, *AtCycD3;1* (Riou-Khamlichi et al., 1999) and *NtKIS1a* were overexpressed simultaneously in plants in two ways. Our phenotypic analyses revealed that overexpression of *NtKIS1a* together with *AtCycD3;1* restored normal plant development. Regarding the leaf phenotype, both the serration and/or undulation observed in NtKIS1a lines and the curling of AtCycD3;1 line disappeared in double overexpressing plants (Fig. 6C). This leaf phenotype restoration was also confirmed at the cellular level, since in double overexpressing plants, cell areas could be described by three categories such as in WT (Fig. 4E; Fig. 6D). Furthermore, several other traits were addressed in the double overexpressing plants (cell shape, plant and organ size, flowering time; not shown) and all converged on the WT phenotype restoration. Consequently, one interpretation would be that the enhanced inhibitory activity brought by *NtKIS1a* overexpression, would allow compensation of the hyperproliferative properties associated with *AtCycD3;1* overexpression. As already mentioned above for animals, D-cyclins control the activity of CDK/cyclin E, responsible for S phase entry, via titration of CIP/KIP (Sherr and Roberts, 1999). Although E-cyclins have not yet been found in plants, a member of the D-cyclin family (cyclin δ2) has some characteristics in common with E-cyclins (Soni et al., 1995). Thus, a second interpretation could be that NtKIS1a would be sequestrated by AtCycD3;1, allowing the activation of putative E-cyclins and then re-activation of mitotic activity. To summarise, our findings indicate that NtKIS1a and AtCycD3;1 function to antagonise each other and this represents the first demonstration in planta of co-operation between a cell cycle inhibitor, NtKIS1a, and a cell cycle activator, AtCycD3;1.

We are grateful to P. Ratet for providing the *Agrobacterium tumefaciens* strain HBA10S, to C. Gatz for providing the Bin-Hyg-TX vector and to O. Grandjean for allowing us the access to the optimas 6.0 software. We thank J. A. H. Murray and R. Stevens for their critical reading of the manuscript, M. Delarue for her helpful criticisms, J. P. Barès and G. Santé for taking care of the plants and R. Boyer for photography. S.G. was supported by a grant from the French MENRT.

References

Azzi, L., Meijer, L., Reed, S. I., Pidikiti, R. and Tung, H. Y. (1992). Interaction between the cell-cycle-control proteins p34cdc2 and p9CKShs2. Evidence for two cooperative binding domains in p9CKShs2. *Eur. J. Biochem.* **203**, 353-360.

Bechtold, N. and Pelletier, G. (1998). In planta Agrobacterium-mediated transformation of adult *Arabidopsis thaliana* plants by vacuum infiltration. *Methods Mol. Biol.* **82**, 259-266.

Bergounioux, C., Brown, S. C. and Petit, P. X. (1992). Flow cytometry and plant protoplast cell biology. *Physiol. Plant.* **85**, 374-386.

Chandra Sekhar, K. N. and Sawhney, V. K. (1991). Regulation of leaf shape in the solanifolia mutant of tomato (*Lycopersicon esculentum*) by plant growth substances. *Ann. Bot.* **67**, 3-6.

Chen, I. T., Akamatsu, M., Smith, M. L., Lung, F. D., Duba, D., Roller, P. P., Fornace, A. J., Jr and O'Connor, P. M. (1996). Characterization of p21Cip1/Waf1 peptide domains required for cyclin E/Cdk2 and PCNA interaction. *Oncogene* **12**, 595-607.

Church, G. M. and Gilbert, W. (1984). Genomic sequencing. *Proc. Natl. Acad. Sci. USA* **81**, 1991-1995.

Cobrinik, D., Lee, M. H., Hannon, G., Mulligan, G., Bronson, R. T., Dyson, N., Harlow, E., Beach, D., Weinberg, R. A. and Jacks, T. (1996). Shared role of the pRB-related p130 and p107 proteins in limb development. *Genes Dev.* **10**, 1633-1644.

De Veylder, L., de Almeida Engler, J., Burssens, S., Manevski, A., Lescure, B., Van Montagu, M., Engler, G. and Inze, D. (1999). A new D-type cyclin of *Arabidopsis thaliana* expressed during lateral root primordia formation. *Planta* **208**, 453-462.

De Veylder, L., Beeckman, T., Beemster, G. T., Krols, L., Terras, F., Landrieu, I., van der Schueren, E., Maes, S., Naudts, M. and Inze, D. (2001). Functional analysis of cyclin-dependent kinase inhibitors of *Arabidopsis*. *Plant Cell* **13**, 1653-1668.

Fero, M. L., Rivkin, M., Tasch, M., Porter, P., Carow, C. E., Firpo, E., Polyak, K., Tsai, L. H., Broudy, V., Perlmutter, R. M. et al. (1996). A syndrome of multiorgan hyperplasia with features of gigantism, tumorigenesis, and female sterility in p27(Kip1)-deficient mice. *Cell* **85**, 733-744.

Galbraith, D. W., Harkins, K. R., Maddox, J. M., Ayres, N. M., Sharma, D. P. and Firoozabady, E. (1983). Rapid flow cytometric analysis of the cell cycle in intact plant tissues. *Science* **220**, 1049-1051.

Geng, Y., Yu, Q., Sicinska, E., Das, M., Bronson, R. T. and Sicinski, P. (2001). Deletion of the p27Kip1 gene restores normal development in cyclin D1- deficient mice. *Proc. Natl. Acad. Sci. USA* **98**, 194-199.

Hattori, N., Davies, T. C., Anson-Cartwright, L. and Cross, J. C. (2000). Periodic expression of the cyclin-dependent kinase inhibitor p57(Kip2) in trophoblast giant cells defines a G2-like gap phase of the endocycle. *Mol. Biol. Cell* **11**, 1037-1045.

Hong, Y., Roy, R. and Ambros, V. (1998). Developmental regulation of a cyclin-dependent kinase inhibitor controls postembryonic cell cycle progression in Caenorhabditis elegans. *Development* **125**, 3585-3597.

Joubes, J. and Chevalier, C. (2000). Endoreduplication in higher plants. *Plant Mol. Biol.* **43**, 735-745.

Koornneef, M. (1994). General genetics. In *Arabidopsis* (ed. E. M. Meyerowitz and C. R. Somerville), pp. 89-120. Plainview, NY: Cold Spring Harbor Laboratory Press.

Larkins, B. A., Dilkes, B. P., Dante, R. A., Coelho, C. M., Woo, Y. and Liu, Y. (2001). Investigating the hows and whys of DNA endoreduplication. *J. Exp. Bot.* **52**, 183-192.

Meijer, M. and Murray, J. A. H. (2000). The role and regulation of D-type cyclins in the plant cell cycle. *Plant Mol. Biol.* **43**, 621-633.

Meijer, M. and Murray, J. A. (2001). Cell cycle controls and the development of plant form. *Curr. Opin. Plant Biol.* **4**, 44-49.

Myster, D. L. and Duronio, R. J. (2000). To differentiate or not to differentiate? *Curr. Biol.* **10**, 302-304.

Ohnuma, S., Philpott, A., Wang, K., Holt, C. E. and Harris, W. A. (1999). p27Xic1, a Cdk inhibitor, promotes the determination of glial cells in *Xenopus* retina. *Cell* **99**, 499-510.

Riou-Khamlichi, C., Huntley, R., Jacqmard, A. and Murray, J. A. (1999). Cytokinin activation of *Arabidopsis* cell division through a D-type cyclin. *Science* **283**, 1541-1544.

Riou-Khamlichi, C., Menges, M., Healy, J. M. and Murray, J. A. (2000). Sugar control of the plant cell cycle: differential regulation of *Arabidopsis* D-type cyclin gene expression. *Mol. Cell Biol.* **20**, 4513-4521.

Russo, A. A., Jeffrey, P. D., Patten, A. K., Massague, J. and Pavletich, N. P. (1996). Crystal structure of the p27Kip1 cyclin-dependent-kinase inhibitor bound to the cyclin A-Cdk2 complex. *Nature* **382**, 325-331.

Sherr, C. J. (1995). D-type cyclins. *Trends Biochem. Sci.* **20**, 187-190.

Sherr, C. J. and Roberts, J. M. (1999). CDK inhibitors: positive and negative regulators of G1-phase progression. *Genes Dev.* **13**, 1501-1512.

Sicinski, P., Donaher, J. L., Parker, S. B., Li, T., Fazeli, A., Gardner, H., Haslam, S. Z., Bronson, R. T., Elledge, S. J. and Weinberg, R. A. (1995). Cyclin D1 provides a link between development and oncogenesis in the retina and breast. *Cell* **82**, 621-630.

Soni, R., Carmichael, J. P., Shah, Z. H. and Murray, J. A. (1995). A family of cyclin D homologs from plants differentially controlled by growth regulators and containing the conserved retinoblastoma protein interaction motif. *Plant Cell* **7**, 85-103.

Stals, H. and Inze, D. (2001). When plant cells decide to divide. *Trends Plant. Sci.* **6**, 359-364.

Tong, W. and Pollard, J. W. (2001). Genetic evidence for the interactions of cyclin D1 and p27(Kip1) in mice. *Mol. Cell Biol.* **21**, 1319-1328.

Traas, J., Hulskamp, M., Gendreau, E. and Hofte, H. (1998). Endoreduplication and development: rule without dividing? *Curr. Opin. Plant Biol.* **1**, 498-503.

Trehin, C., Planchais, S., Glab, N., Perennes, C., Tregear, J. and Bergounioux, C. (1998). Cell cycle regulation by plant growth regulators: involvement of auxin and cytokinin in the re-entry of Petunia protoplasts into the cell cycle. *Planta* **206**, 215-224.

Wang, H., Qi, Q., Schorr, P., Cutler, A. J., Crosby, W. L. and Fowke, L. C. (1998). ICK1, a cyclin-dependent protein kinase inhibitor from *Arabidopsis thaliana* interacts with both Cdc2a and CycD3, and its expression is induced by abscisic acid. *Plant J.* **15**, 501-510.

Wang, H., Zhou, Y., Gilmer, S., Whitwill, S. and Fowke, L. C. (2000). Expression of the plant cyclin-dependent kinase inhibitor ICK1 affects cell division, plant growth and morphology. *Plant J.* **24**, 613-623.

Zhang, P., Wong, C., DePinho, R. A., Harper, J. W. and Elledge, S. J. (1998). Cooperation between the Cdk inhibitors p27(KIP1) and p57(KIP2) in the control of tissue growth and development. *Genes Dev.* **12**, 3162-3167.

Zhang, P., Wong, C., Liu, D., Finegold, M., Harper, J. W. and Elledge, S. J. (1999). p21(CIP1) and p57(KIP2) control muscle differentiation at the myogenin step. *Genes Dev.* **13**, 213-224.